

Understanding the Structure/Activity Relationships of the Iron Regulatory Peptide Hepcidin

Richard J. Clark,^{1,*} Chia Chia Tan,¹ Gloria C. Preza,² Elizabeta Nemeth,² Tomas Ganz,² and David J. Craik¹

¹The University of Queensland, Institute for Molecular Bioscience, Brisbane, Queensland 4072, Australia

²David Geffen School of Medicine, University of California, Los Angeles, Los Angeles, CA 90095, USA

*Correspondence: richard.clark@uq.edu.au

DOI 10.1016/j.chembiol.2010.12.009

SUMMARY

The peptide hormone hepcidin is a key homeostatic regulator of iron metabolism and involved in pathological regulation of iron in response to infection, inflammation, hypoxia, and anemia. It acts by binding to the iron exporter ferroportin, causing it to be internalized and degraded; however, little is known about the structure/activity relationships of the interaction of hepcidin with ferroportin. We show that there are key residues in the N-terminal region of hepcidin that influence its interaction with ferroportin, and we explore the structure/function relationships at these positions. A series of hepcidin mutants in which disulfide bonds were replaced with diselenide bonds showed no change in activity compared to native hepcidin. These results identify important constraints for the development of hepcidin congeners for the treatment of hereditary iron overload.

INTRODUCTION

The peptide hormone hepcidin is a key regulator of iron homeostasis and is produced by the liver in response to high plasma iron levels and inflammatory stimuli (Ganz, 2008; Nemeth and Ganz, 2006). Ferroportin is the sole cellular iron exporter and is expressed on the surface of intestinal enterocytes, macrophages, hepatocytes, and placenta where it releases cellular iron into the plasma (Donovan, et al., 2005). Hepcidin acts by binding to ferroportin, causing the transporter to be internalized and degraded (Nemeth, et al., 2004). The rate of iron efflux from these cells is proportional to the level of ferroportin on the cell membranes. Therefore, hepcidin-induced degradation of ferroportin results in a decrease in the circulating levels of iron within the body.

Hepcidin is synthesized as an 84 amino acid prepropeptide that is subsequently processed to the mature 25 residue peptide, which contains eight cysteines, linked to form four disulfide bonds (Figure 1) (Krause, et al., 2000; Park, et al., 2001). The connectivity of these disulfide bonds was originally proposed, based on a detailed NMR analysis, to be in a Cys7 to Cys23, Cys10 to Cys22, Cys11 to Cys19, and Cys13 to Cys14 ladder-like arrangement that includes a rare vicinal disulfide bond (between Cys 13 and 14) (Hunter, et al., 2002). A later structural study on bass hepcidin reported the same disulfide connectivity

(Lauth, et al., 2005). However, recently it has been shown, using NMR, disulfide mapping, and X-ray crystallography, that this connectivity is apparently incorrect and that, instead, the disulfides form a different connectivity that shares two of the disulfides from the originally proposed connectivity, Cys7 to Cys23 and Cys11 to Cys19, but the vicinal disulfide is absent, and the other two disulfide bonds are located between Cys10 and Cys13 and Cys14 and Cys22 (Jordan, et al., 2009). In this structure hepcidin forms a β -hairpin-like motif containing a central core crosslinked by disulfides and a flexible six residue N-terminal region. It was shown that at physiological temperature, hepcidin interconverts between two conformations (Jordan, et al., 2009). NMR studies at lower and higher temperatures showed that the conformational variation occurs predominantly around the β -hairpin region of the peptide and that the N-terminal region is flexible at all temperatures. The physiological role, if any, of this conformational flexibility remains unclear.

Hepcidin is deactivated by cleavage of the N-terminal region of the molecule, as indicated by the presence of a 20 residue inactive form of hepcidin isolated from urine (Park, et al., 2001). The N-terminal region of hepcidin is essential for binding to ferroportin because sequential truncation of the N-terminal residues results in a progressive loss in activity of the peptide, yet the N-terminal region alone is not sufficient to induce ferroportin internalization (Nemeth, et al., 2006). In addition it has been shown that Cys326 of ferroportin is required for the interaction between hepcidin and ferroportin, which raises the possibility that, among other explanations, a disulfide bond might form between hepcidin and ferroportin (Fernandes, et al., 2009).

Hepcidin dysregulation results in a number of disease states. Hemochromatosis is a genetic condition characterized by abnormally high levels of circulating iron, resulting in iron deposition and subsequent organ damage (Alexander and Kowdley, 2009). Most forms of hemochromatosis result from a deficiency in hepcidin production, and therefore, it should be possible to treat hemochromatosis by administration of synthetic hepcidin or a hepcidin analog. At the other extreme, in anemia of chronic disease associated with chronic infection or inflammation, high hepcidin levels limit the availability of iron for hemoglobin synthesis. Here, antagonists of hepcidin might be therapeutically useful in correcting the iron imbalance.

A key element in the potential development of hepcidin-based treatments for iron regulatory disorders is an understanding of the structure/activity relationships of hepcidin and its interaction with ferroportin. In this study we undertake mutational studies on the N-terminal residues of hepcidin to elucidate these relationships. As our initial approach we performed an alanine scan to

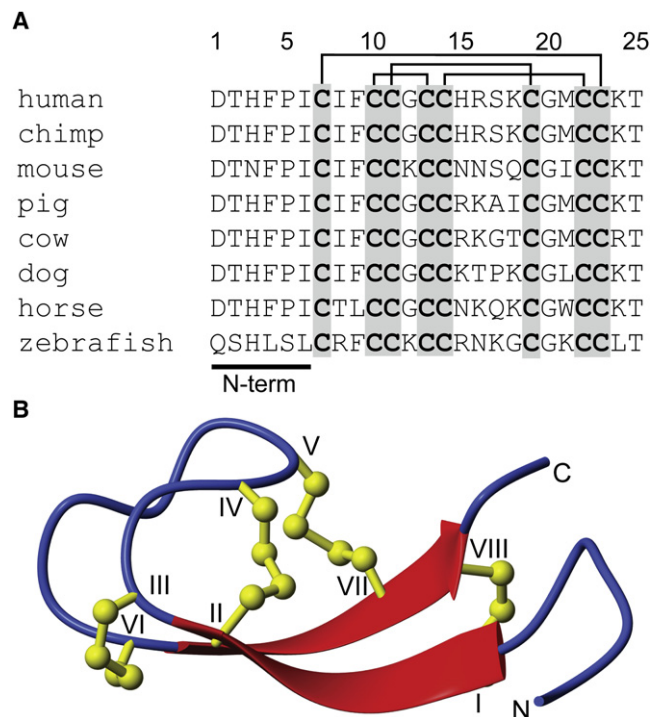


Figure 1. Sequences and Three-Dimensional Structure of Hepcidin

(A) Sequence alignment of selected hepcidin sequences illustrating the high sequence conservation and the N-terminal region essential for biological activity. The sequences contain eight conserved cysteines that form four disulfide bonds, indicated by the lines above the sequence list.

(B) A ribbon depiction of the three-dimensional structure of hepcidin showing the β sheet structure (broad arrows) and the four disulfide bonds (ball and sticks).

determine the specific residues within the N terminus of hepcidin that are involved in its interaction with ferroportin. We subsequently explored the important structural and chemical features required at each of the key positions identified from the alanine scan to establish the structure/activity profile of the critical N terminus of hepcidin. A series of selenocysteine mutants were also examined in an attempt to determine the role of disulfide exchange in the hepcidin/ferroportin interaction. These studies have provided a mechanistic insight into the binding mode of hepcidin with ferroportin.

RESULTS

Peptide Synthesis

The synthesis of the hepcidin analogs for the structure/activity studies was undertaken in two rounds. The first round involved the synthesis of a series of alanine mutants in which each residue of the N-terminal region was individually replaced with alanine. The second round of analogs was based on bioactivity data (described below) and involved mutations of residues His3, Phe4, and Ile6. All analogs were successfully synthesized via solid-phase synthesis methods utilizing Fmoc chemistry. After assembly and cleavage from the resin using TFA, the peptides were oxidized in phosphate buffer containing guanidine, EDTA,

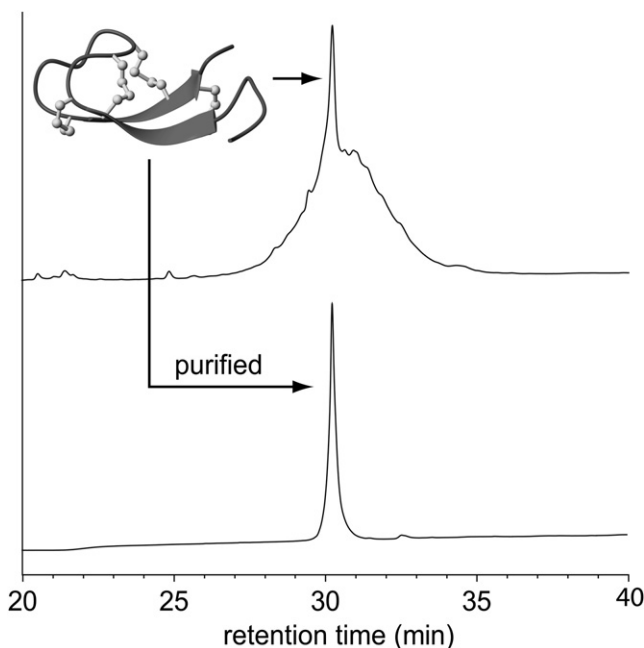


Figure 2. Oxidation and Purification of the Hepcidin Analogs

Oxidation of the reduced hepcidin analogs results in a complex mixture of disulfide isomers, but typically with one predominant species (top). This major isomer for each analog was successfully purified by RP-HPLC (bottom) for structural analysis by NMR and bioactivity assays. The example shown is for the I6K mutant.

cysteine, and cystine to yield a complex mixture of disulfide isomers, as illustrated by the RP-HPLC trace of the crude oxidation mixture shown in Figure 2. Despite this complexity, we were able to isolate, in high purity, a major isomer for 24 of the 26 analogs synthesized (Figure 2). Each of these isomers was analyzed by NMR spectroscopy to confirm that they possessed the native hepcidin fold. Two of the analogs synthesized, F9K and G20F, could not be successfully oxidized to a native-like molecule. These two mutations were originally chosen because of the high sequence conservation at these positions and their proximity to the N-terminal region, and therefore, we believed that they might play a role in the biological activity of hepcidin. However, our results suggest that Phe9 and Gly20 might be conserved because they are important for the correct folding of hepcidin.

Six selenocysteine analogs of hepcidin were designed, i.e., [C7U,C23U]hepcidin, [C10U,C13U]hepcidin, [C11U,C19U]hepcidin, [C14U,C22U]hepcidin, [C7U,C10U,C13U,C23U]hepcidin (Sec₄), and [C7U,C10U,C11U,C13U,C14U, C19U,C22U,C23U] hepcidin (Sec₈), with the aim of elucidating the role of one or more of the disulfide bonds of hepcidin in a potential disulfide exchange with ferroportin. Due to the low pK_a and highly negative redox potential of selenocysteine, the formation of a diselenide bond is favored over a mixed selenylsulfide; furthermore, diselenides are highly resistant to reduction by thiols (Armishaw, et al., 2006; Muttenthaler and Alewood, 2008). Therefore, if one of the hepcidin disulfide bonds underwent exchange with ferroportin, replacing it with a diselenide would result in a loss of activity because it would be unlikely to form a selenylsulfide

bond with the free thiol of the ferroportin Cys326 residue. The selenocysteine analogs of hepcidin were synthesized by solid-phase peptide synthesis using BOC chemistry. The peptides were cleaved from the resin using hydrofluoric acid and during this process generated peptide in which the selenocysteines were oxidized as expected (Muttenthaler and Alewood, 2008). The remaining cysteines were then oxidized under the same conditions used for the structure/activity analogs. Interestingly, the [Sec₈]hepcidin analog, in which all the cysteines are replaced with selenocysteine, folded into a single major oxidized product in hydrofluoric acid during the resin cleavage reaction that was subsequently shown by NMR to be the native isomer. The peptides were then purified by RP-HPLC and analyzed by NMR to confirm that they were correctly folded.

NMR Studies

NMR spectroscopy was used to confirm that the hepcidin analogs all possessed a native fold. $\text{NH}_i\text{-NH}_{i+1}$, $\alpha\text{H}_i\text{-NH}_{i+1}$, and $\beta\text{H}_i\text{-NH}_{i+1}$ connectivities obtained from the NOESY spectrum for each analog were used in the sequential assignment of individual spin systems determined from the TOCSY spectrum. Sequential $\alpha\text{H}_i\text{-NH}_{i+1}$ connectivities were seen for the entire peptide chain except for residues 14–15, which were not visible in the spectra, and at Pro5. The absence of residues Cys14 and His15 is consistent with a similar observation for the native peptide (Hunter, et al., 2002; Jordan, et al., 2009). The presence of $\alpha\text{H}_i\text{-}\delta\text{H}_{i+1}$ NOE correlations indicated that Pro5 was in a *trans* configuration in all analogs.

Secondary αH chemical shifts are the difference between an observed αH chemical shift and that of the corresponding residue in a random coil peptide. A comparison of secondary αH shifts between different peptides provides information on the similarity of their structures. Furthermore, an analysis of secondary shift data yields information on the secondary structures present within peptides. Figure 3 shows a comparison between the secondary αH chemical shifts of the six alanine mutants and native hepcidin and highlights the structural similarity between these peptides. Only small local variations in secondary shifts are observed in the N-terminal region around the sites of amino acid substitution in each analog. The trends in shifts for the core of the molecule, which is defined by the cystine framework, are almost identical, including a series of positive secondary shift values from residues 6 to 11 and 17 to 24, consistent with the proposed β -hairpin structure of hepcidin. Similar results were observed for the structural analysis of the position 3, 4, and 6 analogs and the selenocysteine analogs (see Figure S1 available online). Therefore, any changes in biological activity observed are likely to be due to changes in the chemical characteristics of the specific amino acids and not a change in the global structure of the peptides.

Bioactivity of the Hepcidin Analogs

The ability of the hepcidin analogs to induce ferroportin internalization and degradation was assessed by a measurement of the suppression of fluorescence in HEK cells expressing ferroportin-GFP. Peptides (0.3 μM) were added to the cells, and the activity of each mutant was expressed as a percentage of native hepcidin activity (Table 1). The initial screening was performed on the alanine mutants to characterize the effect of mutation of each

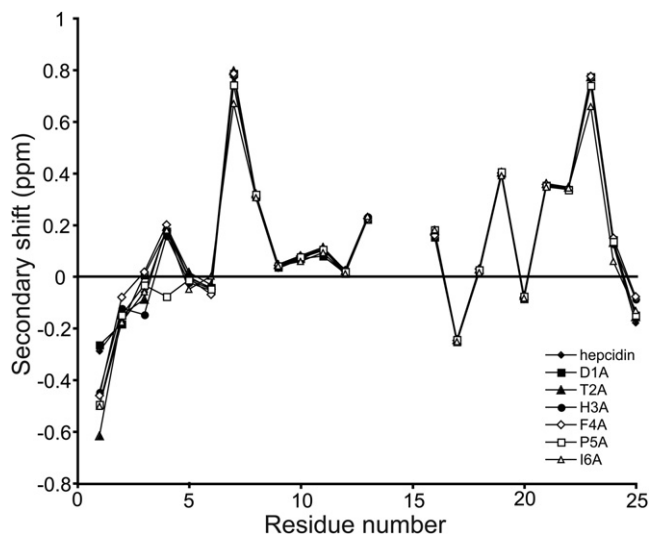


Figure 3. NMR Secondary Shift Analysis of the Alanine Mutants of Hepcidin

All alanine mutants had almost identical αH secondary shift values to native hepcidin except for very small local changes around the site of substitution. A similar trend was observed for all the other hepcidin mutants analyzed in this study (Figure S1).

individual amino acid of the N terminus on activity of the peptide (Figure 4A). Mutation of residues Thr2 to alanine resulted in no significant change in activity compared with native hepcidin, with suppression of fluorescence relative to hepcidin of $88\% \pm 13\%$. A moderate loss in activity was observed on mutation of Asp1 ($68\% \pm 5\%$) and Pro5 ($77\% \pm 3\%$) to alanine. The largest effect was seen when His3, Phe4, or Ile6 was changed to alanine, with these mutants having only $49\% \pm 1\%$, $33\% \pm 18\%$, and $31\% \pm 4\%$, respectively, of the activity of native hepcidin. Therefore, the key residues identified by the alanine scan for the interaction between hepcidin and ferroportin are His3, Phe4, and Ile6.

A second series of analogs was then made to elucidate the specific chemical requirements at each of these positions required for binding of hepcidin to ferroportin (Figures 4B–4D). None of the three positions tolerated the presence of positively or negatively charged residues because substitution of lysine or aspartic acid at any of these positions resulted in almost complete loss in activity. At position 3 (Figure 4B), substitution of the histidine with a phenylalanine ring resulted in an almost fully active peptide ($92\% \pm 0.3\%$), suggesting that the nitrogens in the histidine ring are not required for interaction with the receptor. A tryptophan at position 3 resulted in a substantial loss of activity ($56\% \pm 5\%$), presumably due to the greater bulk of this residue. Changing the stereochemistry by incorporation of a D-histidine resulted in some loss in activity ($73\% \pm 2\%$), which suggests that although the side chain orientation of this residue has some effect, either ferroportin can accommodate this change to some degree, or the flexibility of the N terminus can compensate for the change in stereochemistry. Replacement of Phe4 with a cyclohexylalanine or a norleucine resulted in little or no loss in activity ($88\% \pm 8\%$ and $105\% \pm 11\%$, respectively), indicating that neither an aromatic or ring moiety is required at this position and that a long hydrophobic side chain

Table 1. Bioactivity Data for Hecpudin Analogs Relative to Native Hecpudin

Peptide	Activity Relative to Hecpudin \pm SEM (%) ^a
Hecpudin	100
D1A	67 \pm 5
T2A	88 \pm 13
H3A	49 \pm 1
F4A	33 \pm 18
P5A	77 \pm 3
I6A	31 \pm 4
H3F	92 \pm 0.3
H3W	56 \pm 5
H3h	73 \pm 2
H3Dab	14 \pm 0.1
H3K	9 \pm 2
H3D	7 \pm 6
F4Cha	88 \pm 8
F4Nle	105 \pm 11
F4Y	75 \pm 22
F4f	29 \pm 15
F4K	15 \pm 15
F4D	12 \pm 10
I6F	64 \pm 4
I6i	55 \pm 2
I6K	18 \pm 12
I6D	2 \pm 5
I8K	87 \pm 5
P5O	89 \pm 2

Activity relative to native hecpudin using the GFP-ferroportin assay. Dab, diaminobutyric acid; Cha, cyclohexylalanine; Nle, norleucine; O, hydroxyproline.

^a n = 3–6.

is sufficient for activity (Figure 4C). This suggestion is further supported by the data associated with the introduction of a more polar residue, tyrosine, which causes some loss of activity (75% \pm 22%). The interaction is also stereospecific because substitution with D-phenylalanine results in a peptide with an activity of only 29% \pm 15% relative to hecpudin. Substitution of Ile6 with a phenylalanine leads to a loss in activity (64% \pm 4%), suggesting that a bulkier aromatic ring at this position cannot be accommodated by ferroportin as easily as the branched isoleucine (Figure 4D). Mutation to a D-isoleucine also results in a loss of activity (55% \pm 2%), implying that there is a stereochemical preference for the interaction.

Because the interaction between hecpudin and ferroportin appeared to be dominated by hydrophobic interactions, two additional mutants were synthesized, with Pro5 altered to a hydroxyproline and the highly conserved Ile8 and Phe9 residues to a lysine. Neither the mutation of Pro5 to hydroxyproline or Ile8 to lysine resulted in any substantial loss of hecpudin activity (Table 1). As stated earlier, we were unable to produce a correctly folded F9K mutant.

To examine the role of the disulfide bonds in the interaction between hecpudin and ferroportin, a series of selenocysteine analogs of hecpudin were synthesized and tested for their ability to induce ferroportin internalization and degradation (Figure 5A). Interestingly, all of the diselenide analogs exhibited an almost identical dose-response curve to hecpudin (Figure 5B), suggesting that a thiol exchange between hecpudin and ferroportin is not essential for hecpudin activity. However, reduction/alkylation assays on native and Sec₈ hecpudin revealed that although [Sec₈]hecpudin was more stable to reduction by DTT than native hecpudin, the peptide could still be reduced (Figure S2). Interestingly, if the reaction time was extended, [Sec₈]hecpudin was found to reoxidize, presumably due to exhaustion of DTT in the reaction.

Antagonists of hecpudin have the potential to be used as a treatment for anemia of inflammation, an iron deficiency disease that results from chronic overproduction of hecpudin. Therefore, the less-active mutants synthesized in this study were tested for their ability to act as antagonists of native hecpudin. None of the hecpudin analogs exhibited antagonistic activity against the action of hecpudin in the ferroportin-GFP assay when hecpudin and each analog were coincubated (data not shown).

DISCUSSION

In this study we have characterized the key N-terminal residues of hecpudin involved in its interaction with ferroportin. Figure 6A summarizes the structure/activity data known for hecpudin from natural mutations (Biasiotto, et al., 2003; Jacolot, et al., 2004; Merryweather-Clarke, et al., 2003; Nemeth, et al., 2006), previous studies, (Nemeth, et al., 2006; Nemeth, et al., 2004) and this work. Substitution of His3, Phe4, or Ile6 with alanine resulted in a substantial loss in the ability of the hecpudin mutants to trigger the internalization and degradation of ferroportin. More extensive substitutions at each of these positions revealed that the interaction between hecpudin and ferroportin is dominated by hydrophobic interactions because mutation of any of the identified residues in hecpudin with charged amino acids resulted in a complete loss of activity. Finally, a change in stereochemistry of Phe4 and Ile6 by substitution with the corresponding D amino acid caused a significant loss of activity. This suggests that these interactions are also stereospecific.

Figure 6B maps the structure/activity data onto the molecular surface of hecpudin. It can clearly be seen that His3, Phe4, and Ile6 form a localized patch at one end of the molecule and that this patch is flanked by the other N-terminal residues that have a small to moderate influence on activity. The known natural hecpudin mutant, G21D, and the synthetic mutant, M21Y, exhibit comparable activity to native hecpudin (Nemeth, et al., 2006). Based on the data obtained from this study and truncations of the N terminus (Nemeth, et al., 2006), this finding is not surprising because both these residues are located at the opposite end of the molecule to the activity hot spot. The importance of the N-terminal residues in the interaction of hecpudin with ferroportin is further highlighted by a comparison of mammalian hecpudin sequences. Figure 6C illustrates the fact that the N-terminal residues important for biological activity are among the most highly conserved, whereas residues located away from the activity center, around the β -turn, are less conserved.

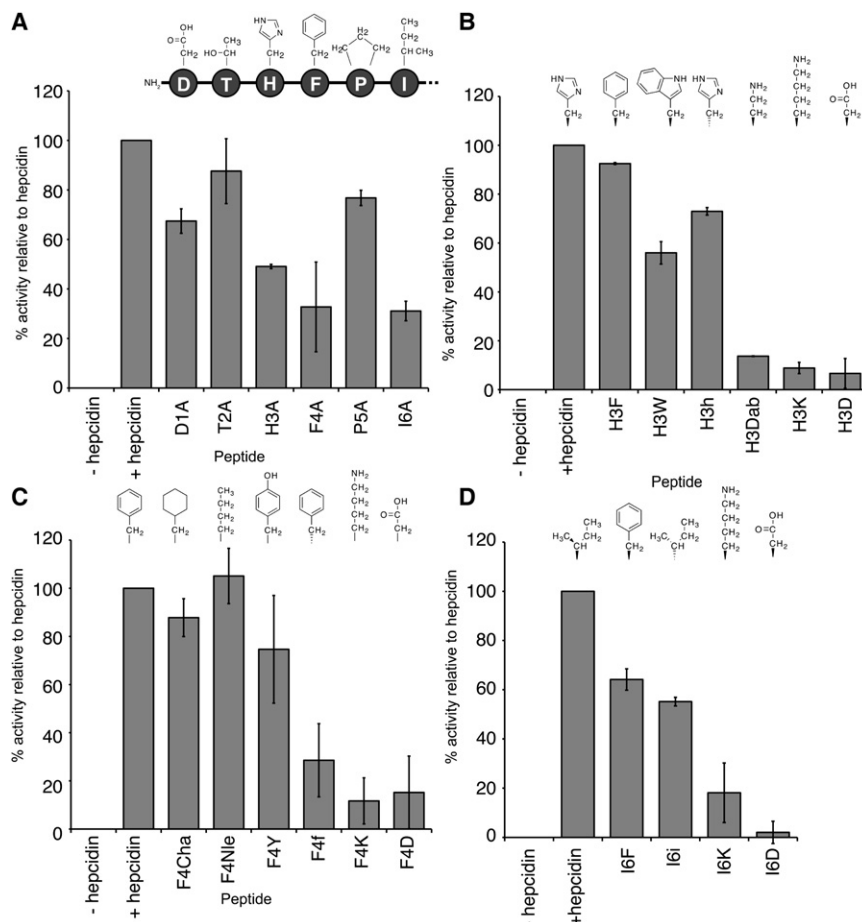


Figure 4. Biological Activity of the Synthetic Hecpudin Mutants

Relative activities of native hecpudin and the alanine mutants (A), His3 mutants (B), Phe4 mutants (C), and Ile6 mutants (D). HEK293T cells stably expressing ferroportin-GFP construct were treated with peptide (0.3 μ M) for 24 hr, and the intensity of green fluorescence was then measured by FACS and expressed as a percentage relative to native hecpudin.

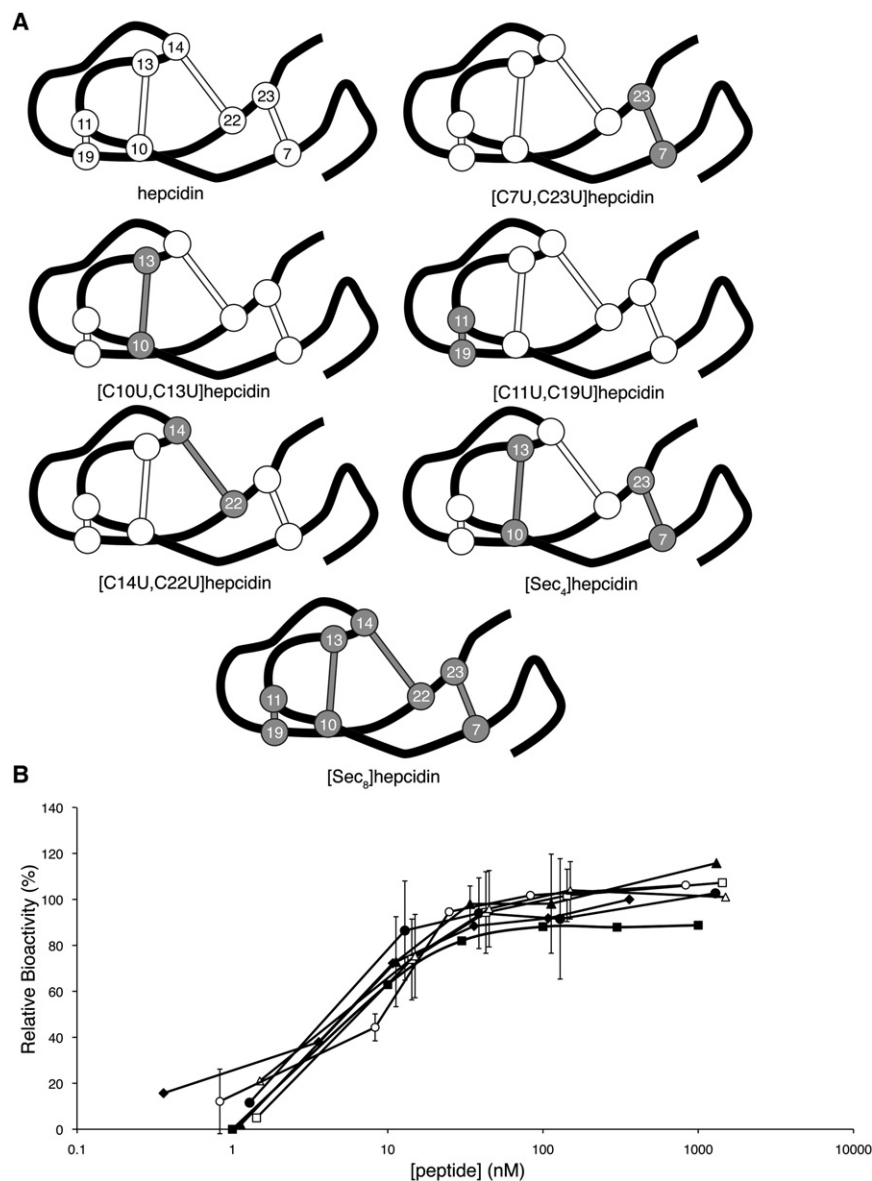
possible to reduce [Sec₈]hecpudin with DTT, and therefore, the occurrence of disulfide exchange between hecpudin and ferroportin cannot be unequivocally resolved.

None of the hecpudin analogs exhibited enhanced activity compared with native hecpudin, a finding that might be due to one of several reasons. First, the ferroportin-GFP degradation assay used is designed to give maximal degradation of ferroportin-GFP when incubated with native hecpudin and, therefore, might only detect mutants with decreased activity. Also, the native hecpudin sequence might be optimized for its interaction with ferroportin, which is supported by the high sequence conservation across species, and therefore, the existing interactions are highly efficient. For example, in the case of Phe4, it appears that this interaction is simply a hydro-

The extracellular loop of ferroportin that interacts with hecpudin has recently been identified from the observation that Cys326 mutation in this loop results in ferroportin being resistant to hecpudin binding (De Domenico, et al., 2005; Fernandes, et al., 2009). It has been proposed that the free thiol of the Cys326 residue forms a disulfide bond with one of the cysteine residues in hecpudin (Fernandes, et al., 2009). We attempted to test this hypothesis by synthesizing a series of diselenide bond mutants of hecpudin. Diselenide bonds are structurally analogous to disulfide bonds but are more resistant to reduction (Armishaw, et al., 2006; Muttenthaler and Alewood, 2008). Therefore, we envisaged that if a hecpudin disulfide bond was involved in a disulfide exchange with ferroportin, replacement of this bond with a diselenide would result in a loss of activity. Diselenide analogs were designed to test the effects of replacing both individual and multiple disulfide bonds, and all peptides were shown to be structurally comparable by NMR secondary shift analysis. This analysis also confirmed the recently revised disulfide connectivity and three-dimensional structure of hecpudin because the [C10U,C13U]hecpudin and [C14U,C22U]hecpudin analogs had identical secondary shifts to native hecpudin (Jordan, et al., 2009). Activity assays revealed that the activity of all the diselenide analogs was comparable to native hecpudin, suggesting that no disulfide exchange occurs between the hecpudin and receptor. However, in reduction trials we found that it was

phobic one that is relatively tolerant to size as long as the correct stereochemistry is maintained. Alternatively, single-point mutations might not be sufficient to enhance activity significantly, and multi-point mutation analogs might be needed to produce a more efficacious hecpudin analog. Finally, it is also possible that there are mutations at these positions that could improve activity that were not synthesized in this study and that the incorporation of unnatural amino acids into the sequence of hecpudin and variation of noncritical amino acids to introduce additional contacts might be avenues to explore for the production of more potent hecpudin analogs.

Hecpudin has an exceptionally high cysteine content relative to other proteins (Fahey, et al., 1977), with eight of the 25 residues being cysteine (~30%). When eight cysteines are present in a peptide, there are 105 possible four-disulfide isomers that can be produced from a random oxidation. Therefore, it is very surprising that it is possible to fold hecpudin in vitro into the native isomer, even in the denaturing conditions used in this study. In a stunning illustration of this robust folding, we observed that correctly folded [Sec₈]hecpudin was formed spontaneously during the hydrofluoric acid cleavage reaction. Presumably, there are interactions between residues within the sequence that drive the correct folding of hecpudin to favor the native disulfide connectivity. Our results show that the F9K and G20F mutations disrupted folding, suggesting that these changes to



the hepcidin sequence introduce interactions unfavorable to formation of the native disulfide isomer.

It is interesting to consider what role the framework of hepcidin plays in its biological function, considering that many of the key residues important for biological activity are localized within the flexible N terminus. It has been shown that the N terminus alone is not sufficient for activity (Nemeth, et al., 2006), which implies a role for other residues within the framework. In addition to the conserved cysteines, which provide structural stability to the molecule and might form an intermolecular disulfide with ferroportin, there are a number of residues within the hepcidin sequence that are conserved across species (Figure 6C), and it is possible that these could be important for either the interaction of hepcidin with ferroportin or might modulate other processes in the internalization mechanism.

Figure 5. Selenocystine Analogs of Hepcidin

(A) Schematic representation of native hepcidin and the selenocystine analogs synthesized in this study. The peptide backbone is represented by the black line, disulfides as the white ball and sticks, and diselenides as the gray ball and sticks. Each disulfide/diselenide is numbered based on its position in the sequence.

(B) Dose-response curve for hepcidin (filled diamonds), [U7C,U23C]hepcidin (filled squares), [C10U,C13U]hepcidin (filled triangles), [C11U,C19U]hepcidin (filled circles), [C14U,C22U]hepcidin (open squares), [Sec₄]hepcidin (open triangles), and [Sec₆]hepcidin (open circles). HEK293T cells stably expressing ferroportin-GFP construct were treated with varying concentrations of peptide for 24 hr, and the intensity of green fluorescence was then measured by FACS.

See also Figure S2.

SIGNIFICANCE

Hepcidin is the major peptide hormone in the body regulating iron levels. There are a number of diseases associated with the dysregulation of hepcidin levels in humans, including hemochromatosis (iron overload) and anemia (low iron levels). This study represents a first step toward defining the hepcidin pharmacophore at the ferroportin-binding site, and the data generated could be crucial in the development of agonists or antagonists for the treatment of iron-related disorders. We have identified the key positions within the N terminus of hepcidin for its ability to trigger internalization and degradation of ferroportin and have elucidated the chemical and structural requirements at each of these positions. Our findings, combined with literature data, have

allowed us to propose a mechanistic model for the hepcidin/ferroportin interaction that we can interrogate in future studies and will be invaluable in the drug development process.

EXPERIMENTAL PROCEDURES

Peptide Synthesis

All peptides were assembled on 2-Cl-2-trityl resin (Novabiochem) by solid-phase peptide synthesis on a Liberty Microwave Peptide Synthesizer using the in situ neutralization/HBTU protocol and Fmoc chemistry (Schnölzer, et al., 1992). Cleavage of the peptides from the resin was achieved using TFA with triisopropylsilane and water as scavengers (9:0.5:0.5 [v/v] TFA:triisopropylsilane:water) at 22°C for 2 hr. The selenocysteine analogs of hepcidin were synthesized with the in situ neutralization/HBTU protocol and Boc chemistry using Boc-Sec(MeBzl)-OH at sites where selenocysteine was replacing cysteine. These peptides were cleaved using HF with *p*-cresol and

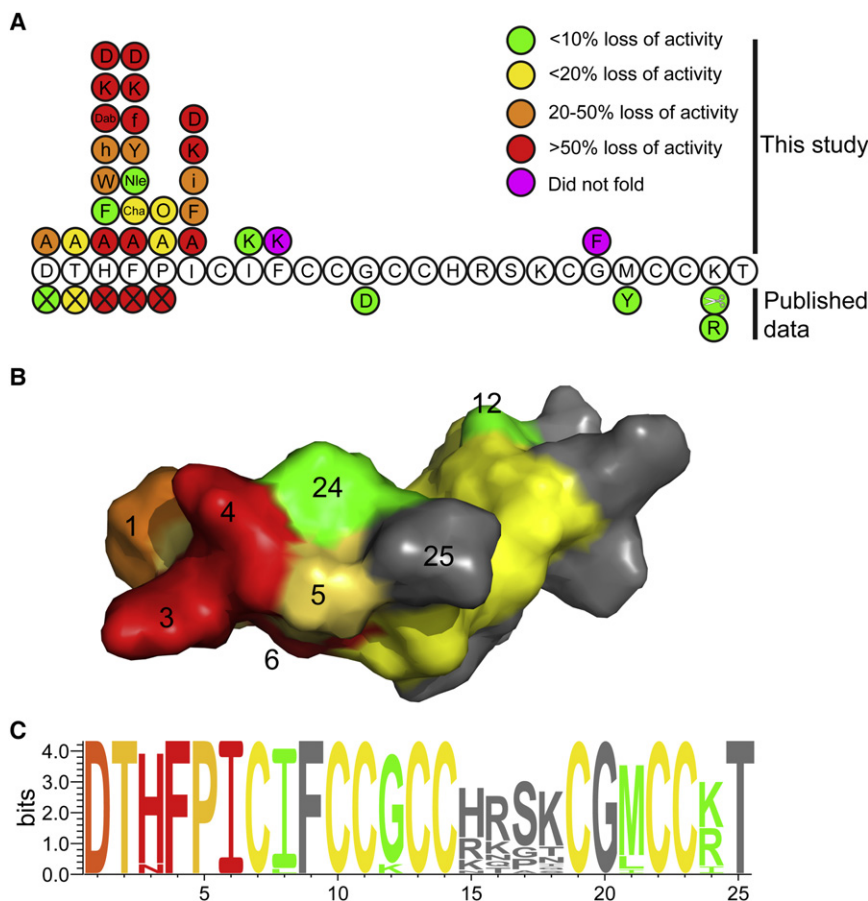


Figure 6. Summary of Structure/Activity Relationships of Hepcidin

(A) The sequence of hepcidin showing the effect on activity of mutations from this study, naturally occurring mutations and truncation of the N-terminal residues (indicated by the X symbol) (Nemeth, et al., 2006). The colors indicate the percent loss in activity relative to hepcidin as follows: green <10% loss in activity, yellow 10%–20% loss, orange 20%–50% loss, and red >50% loss. Mutations shown in magenta are peptides that did not fold.

(B) A surface representation of hepcidin with the surface color coded using the same scheme as (A). The activity data presented are for the alanine mutants plus the known natural mutations. It can be seen that residues His3, Phe4, and Ile6 form a localized patch on the surface of the molecule. The conserved cysteines are colored yellow.

(C) A sequence logo representation (Schneider and Stephens, 1990) of hepcidin, colored using the scheme from (A). The activity data presented are for the alanine mutants together with the known natural mutations and the C-terminal truncation data (Nemeth, et al., 2006). The relative heights of the amino acid symbols at each position represent the degree of sequence conservation at each of these positions. As expected, the residues toward the N-terminal region of the peptide that are important for the interaction of hepcidin are the most highly conserved, whereas those around the β -turn show lower sequence conservation.

p-thiocresol as scavengers (9:0.5:0.5 [v/v]) HF:*p*-cresol:*p*-thiocresol). The reaction was allowed to proceed at -5°C – 0°C for 1.5 hr. The HF was then removed under vacuum and the peptide precipitated with ether, filtered, dissolved in 50% acetonitrile containing 0.05% TFA, and lyophilized. After cleavage, the peptide was precipitated with ether, filtered, and then dissolved in 50% acetonitrile containing 0.05% TFA and lyophilized. Crude peptides were purified by RP-HPLC on a C_{18} column using a gradient of 0%–80% B (A, H_2O /0.05% TFA; B, 90% CH_3CN /10% H_2O /0.045% TFA) in 80 min. Analytical RP-HPLC and ES-MS confirmed the purity and molecular mass of the synthesized peptides.

The reduced peptides were oxidized by incubating in 0.1 M sodium phosphate buffer containing 4 M guanidine, 2 mM EDTA, 3 mM cysteine, and 0.15 mM cystine (pH 7.8) for approximately 18 hr at room temperature. The reaction mixture was purified by RP-HPLC to yield the cyclic/oxidized peptides. Analytical RP-HPLC and ES-MS confirmed the purity of the final products. All hepcidin analogs were stored as lyophilized solids at -20°C .

NMR Studies

Structural data for the hepcidin analogs were obtained using NMR spectroscopy for samples dissolved in 90% H_2O and 10% D_2O at a pH of approximately 4. A Bruker Avance 600 MHz NMR spectrometer was used to acquire spectra, including ^1H , TOCSY, and NOESY data, as described previously (Clark, et al., 2006a, 2006b) and processed using Topspin (Bruker). All spectra were recorded at 298 K. Processed spectra were analyzed and assigned within the program Sparky (Goddard and Kneller, 2008).

Flow Cytometry

ECR293-Fpn, a cell line stably transfected with the mouse ferroportin-GFP construct under the control of ponasterone-inducible promoter, was prepared

and maintained as described previously (Nemeth, et al., 2004). Briefly, cells expressing Fpn-GFP were treated with peptides (0.3 μM) for 24 hr. Peptide concentrations were determined by measurement of absorbance at 214 nm and using a calculated extinction coefficient based on the peptide sequence (Moffatt, et al., 2000). Cells not induced with ponasterone to express Fpn-GFP were used to establish a gate to exclude background fluorescence, and cells induced with ponasterone, but not treated with peptides, were used as the positive control. After treatment with hepcidin or its mutated analogs ($n = 3$ –6), the cells lost fluorescence in proportion to the activity of each peptide. The results were expressed as a fraction of the activity of hepcidin, according to the formula: $1 - [(F_x - F_{\text{hep25}})/(F_{\text{untreated}} - F_{\text{hep25}})]$, where F was the mean fraction of cells within the green fluorescence gate, and x was the peptide.

Antagonist Competition of Hepcidin

ECR293-Fpn, a cell line stably transfected with the mouse ferroportin-GFP construct under the control of ponasterone-inducible promoter, was prepared and maintained as described previously (Nemeth, et al., 2004). Briefly, cells expressing Fpn-GFP were treated with Hep25 (0.717 μM) and with mutant (3.3–3.6 μM) simultaneously for 24 hr.

SUPPLEMENTAL INFORMATION

Supplemental Information includes two figures and can be found with this article online at doi:10.1016/j.chembiol.2010.12.009.

ACKNOWLEDGMENTS

Work in our laboratory on hepcidin is supported by a grant from the National Health and Medical Research Council (NHMRC, ID456073). D.J.C. is a NHMRC

Principal Research Fellow. R.J.C. is a NHMRC Biomedical Career Development Award Fellow. We gratefully acknowledge access to the facilities of the ARC Special Research Centre for Functional and Applied Genomics. Work in the Los Angeles laboratory was supported by NIH grants R01 DK082717 and R01 DK 065029 (T.G., E.N., and G.C.P.).

Received: February 15, 2010

Revised: December 1, 2010

Accepted: December 10, 2010

Published: March 24, 2011

REFERENCES

- Alexander, J., and Kowdley, K.V. (2009). HFE-associated hereditary hemochromatosis. *Genet. Med.* 11, 307–313.
- Armishaw, C.J., Daly, N.L., Nevin, S.T., Adams, D.J., Craik, D.J., and Alewood, P.F. (2006). Alpha-selenoconotoxins, a new class of potent $\alpha 7$ neuronal nicotinic receptor antagonists. *J. Biol. Chem.* 281, 14136–14143.
- Biasotto, G., Belloli, S., Ruggeri, G., Zanella, I., Gerardi, G., Corrado, M., Gobbi, E., Albertini, A., and Arosio, P. (2003). Identification of new mutations of the HFE, hepcidin, and transferrin receptor 2 genes by denaturing HPLC analysis of individuals with biochemical indications of iron overload. *Clin. Chem.* 49, 1981–1988.
- Clark, R.J., Daly, N.L., and Craik, D.J. (2006a). Structural plasticity of the cyclic-cystine-knot framework: implications for biological activity and drug design. *Biochem. J.* 394, 85–93.
- Clark, R.J., Fischer, H., Nevin, S.T., Adams, D.J., and Craik, D.J. (2006b). The synthesis, structural characterization, and receptor specificity of the α -conotoxin Vc1.1. *J. Biol. Chem.* 281, 23254–23263.
- De Domenico, I., Ward, D.M., Nemeth, E., Vaughn, M.B., Musci, G., Ganz, T., and Kaplan, J. (2005). The molecular basis of ferroportin-linked hemochromatosis. *Proc. Natl. Acad. Sci. USA* 102, 8955–8960.
- Donovan, A., Lima, C.A., Pinkus, J.L., Pinkus, G.S., Zon, L.I., Robine, S., and Andrews, N.C. (2005). The iron exporter ferroportin/Slc40a1 is essential for iron homeostasis. *Cell Metab.* 1, 191–200.
- Fahey, R.C., Hunt, J.S., and Windham, G.C. (1977). Cysteine and Cystine Content of Proteins - Differences between Intracellular and Extracellular Proteins. *J. Mol. Evol.* 10, 155–160.
- Fernandes, A., Preza, G.C., Phung, Y., De Domenico, I., Kaplan, J., Ganz, T., and Nemeth, E. (2009). The molecular basis of hepcidin-resistant hereditary hemochromatosis. *Blood* 114, 437–443.
- Ganz, T. (2008). Iron homeostasis: fitting the puzzle pieces together. *Cell Metab.* 7, 288–290.
- Goddard, T.D., and Kneller, D.G. (2008). SPARKY 3 (computer program). (San Francisco, CA: University of California, San Francisco).
- Hunter, H.N., Fulton, D.B., Ganz, T., and Vogel, H.J. (2002). The solution structure of human hepcidin, a peptide hormone with antimicrobial activity that is involved in iron uptake and hereditary hemochromatosis. *J. Biol. Chem.* 277, 37597–37603.
- Jacotot, S., Le Gac, G., Scotet, V., Quere, I., Mura, C., and Ferec, C. (2004). HAMP as a modifier gene that increases the phenotypic expression of the HFE pC282Y homozygous genotype. *Blood* 103, 2835–2840.
- Jordan, J.B., Poppe, L., Haniu, M., Arvedson, T., Syed, R., Li, V., Kohno, H., Kim, H., Schnier, P.D., Harvey, T.S., et al. (2009). Heparin revisited, disulfide connectivity, dynamics, and structure. *J. Biol. Chem.* 284, 24155–24167.
- Krause, A., Neitz, S., Magert, H.J., Schulz, A., Forssmann, W.G., Schulz-Knappe, P., and Ademann, K. (2000). LEAP-1, a novel highly disulfide-bonded human peptide, exhibits antimicrobial activity. *FEBS Lett.* 480, 147–150.
- Lauth, X., Babon, J.J., Stannard, J.A., Singh, S., Nizet, V., Carlberg, J.M., Ostland, V.E., Pennington, M.W., Norton, R.S., and Westerman, M.E. (2005). Bass hepcidin synthesis, solution structure, antimicrobial activities and synergism, and in vivo hepatic response to bacterial infections. *J. Biol. Chem.* 280, 9272–9282.
- Merryweather-Clarke, A.T., Cadet, E., Bomford, A., Capron, D., Viprakasit, V., Miller, A., McHugh, P.J., Chapman, R.W., Poynton, J.J., Wilmhurst, V.L., et al. (2003). Digenic inheritance of mutations in HAMP and HFE results in different types of haemochromatosis. *Hum. Mol. Genet.* 12, 2241–2247.
- Moffatt, F., Senkars, P., and Ricketts, D. (2000). Approaches towards the quantitative analysis of peptides and proteins by reversed-phase high-performance liquid chromatography in the absence of a pure reference sample. *J. Chromatogr. A* 891, 235–242.
- Muttenthaler, M., and Alewood, P.F. (2008). Seleoneptide chemistry. *J. Pept. Sci.* 14, 1223–1230.
- Nemeth, E., and Ganz, T. (2006). Regulation of iron metabolism by hepcidin. *Annu. Rev. Nutr.* 26, 323–342.
- Nemeth, E., Tuttle, M.S., Powelson, J., Vaughn, M.B., Donovan, A., Ward, D.M., Ganz, T., and Kaplan, J. (2004). Heparin regulates cellular iron efflux by binding to ferroportin and inducing its internalization. *Science* 306, 2090–2093.
- Nemeth, E., Preza, G.C., Jung, C.L., Kaplan, J., Waring, A.J., and Ganz, T. (2006). The N-terminus of hepcidin is essential for its interaction with ferroportin: structure-function study. *Blood* 107, 328–333.
- Park, C.H., Valore, E.V., Waring, A.J., and Ganz, T. (2001). Heparin, a urinary antimicrobial peptide synthesized in the liver. *J. Biol. Chem.* 276, 7806–7810.
- Schneider, T.D., and Stephens, R.M. (1990). Sequence logos: a new way to display consensus sequences. *Nucleic Acids Res.* 18, 6097–6100.
- Schnölzer, M., Alewood, P., Jones, A., Alewood, D., and Kent, S.B.H. (1992). In situ neutralization in Boc-chemistry solid phase peptide synthesis. *Int. J. Pept. Protein Res.* 40, 180–193.